Human Body Size and Shape Effect on UWB On-Body WBAN Radio Channels - Preliminary Results

Timo Kumpuniemi
Centre for Wireless Communications, P.O. Box 4500
FI-90014 University of Oulu, FINLAND
+358 294 482 882
timo.kumpuniemi@ee.oulu.fi

Matti Hämäläinen
Centre for Wireless Communications, P.O. Box 4500
FI-90014 University of Oulu, FINLAND
+358 294 482 856
matti.hamalainen@ee.oulu.fi

Kamya Yekeh Yazdandoost
Centre for Wireless Communications, P.O. Box 4500
FI-90014 University of Oulu, FINLAND
+358 294 487 623
yazdandoost@ee.oulu.fi

Jari Iinatti
Centre for Wireless Communications, P.O. Box 4500
FI-90014 University of Oulu, FINLAND
+358 294 482 822
jari.iinatti@ee.oulu.fi

ABSTRACT
This paper examines differences between wireless ultra wideband radio channels when various test persons are measured. The work bases on static on-body measurements conducted in an anechoic chamber at the frequency range of 2-8 GHz by using a vector network analyzer. Three male and one female test persons were measured. The study was repeated by using two different planar antenna types: dipole and double loop that were attached to four antennas positions on the body. From the resulted frequency domain data, the corresponding time-domain channel impulse responses (CIRs) were solved. First, the path losses of the first arriving paths were compared. Depending on the link type, the path losses behaved differently between the test persons. The average path loss exponent was noted to decrease as the body size increased. The results of the male and female with the same body sizes are similar. Secondly, the excess delays of the CIRs were found out. The excess delay increases with larger body sizes among the males. The female has similar result as the largest male. The dipole antenna has, on the average, longer excess delay than the double loop. Finally, the examination of the cross-correlations between the channels show higher values as the body size is increased. No difference exists between the genders with the same body sizes.

Categories and Subject Descriptors
J.2 [**Physical Sciences and Engineering**]: – *electronics, engineering, physics.*

General Terms
Measurement, Experimentation.

Keywords
Body area network, radio channel, ultra wideband.

1. INTRODUCTION
For quite a long time, a discussion of using wireless body area network (WBAN) communications in the medical field has existed. The interest is increasing, as the mean age of population in many developed countries is constantly growing [1,2]. This forces the nations to organize their medical operations in a more cost effective way. WBAN technologies enable the use of varioussensors on the person's body (on-body), in the vicinity of it (off-body) or inside the body (in-body) [3]. They ease the work load of the medical staff by enabling, e.g., the remote monitoring of the patients either in hospitals or homes. The latter gives the opportunity for the patients to live longer in their familiar environment increasing their quality of lives. The non-existence of wires is convenient for both the patients and the medical staff.

One highly suitable solution for short range communications, as in WBANs, is the ultra wideband (UWB) technique. In 2012, the Institute of Electrical and Electronics Engineers (IEEE) published a standard called IEEE 802.15.6 [4]. In it, the impulse radio UWB technique is defined to be the mandatory physical layer waveform to be used in WBANs in the frequency bands of 3.2448-4.7424 GHz and 6.24-10.2336 GHz.

The variances in the on-body UWB channels between different test persons are examined in this paper. The results are based on static frequency domain measurements done with a vector network analyzer (VNA) in an anechoic chamber in the frequency range of 2-8 GHz. Four test persons are under examination: one female and three males. The work was repeated by using two different planar antenna types: dipole and double loop antennas. The measurement data is post-processed to obtain the corresponding time-domain channel impulse responses (CIRs), out of which the differences in the attenuation of the first arriving path, the slope of the CIR decay and the CIR excess delays were solved. Also the path loss characteristics are evaluated. The work is a part of a larger UWB WBAN research initiative, whose other results are reported in [5-7].

2. MEASUREMENT SETUP
The test persons were located in a 60 m^2 large electromagnetic compatibility room, in which an anechoic chamber with a floor size of 245 cm by 365 cm was formed by using movable absorber blocks. The measured persons were wearing cotton T-shirts and jeans, whereas shoes, rings, belts, glasses and other easily undressable articles containing metal were removed.

The utilized VNA type was Rohde & Schwartz ZVA8 with four test ports. Eight meters long Huber + Suhner SUCOFLEX

Permission to make digital or hard copies of all or part of this work for personal or classroom use is granted without fee provided that copies are not made or distributed for profit or commercial advantage and that copies bear this notice and the full citation on the first page. To copy otherwise, to republish, to post on servers or to redistribute to lists, requires prior specific permission and/or a fee.
UWBAN 2014, September 29-October 01, London, Great Britain
Copyright © 2014 ICST 978-1-63190-047-1
DOI 10.4108/icst.bodynets.2014.256996

104PEA measurement cables were connected to the ports enabling the placement of the VNA outside the chamber. The device was controlled by a laptop using LabVIEW software. One hundred consecutive frequency sweeps containing 1601 frequency points were recorded for each link, and both the forward and reverse links were stored. The transmit power of the VNA was set to a value of +10 dBm. The measurement setup is elaborated more in [5,6]. The planar dipole and double loop antennas used in the work are shown in Fig. 1, where the ruler scale is in centimeters. Their structures, dimensions and performances are described in detail in [8,9].

3. CONDUCTED MEASUREMENTS

3.1 Test Persons

The three male test persons were selected to represent different heights in order to be able to compare the effect of different body dimensions. The fourth female test person was selected to have similar height with one of the males in order to compare the effect of the gender. The parameters describing the test persons are gathered in Table 1. The body mass index (BMI) B is calculated based on the person's height and mass by using the formula

$$B = m/h^2, \tag{1}$$

where m is the mass in kilograms and h is the height in meters [10]. Test person B was in his late twenties, test persons A and D in their mid-thirties and test person C in his late forties at the time of the measurements.

3.2 Measured Radio Links

Four antenna locations on the test persons' bodies shown in Fig. 2 were selected. The frequency responses between the antennas were measured. On the frontal body, spots on the abdomen (AB), on the right wrist (RW) and left ankle (LA) are visible. On the back side of the body, the spot on the lumbar region on the back (BA) was selected. The spot (LA) is the same as seen on the frontal body figure. Between the antennas and the body, pieces of material called ROHACELL 31 HF [11] with a thickness of 20 mm were installed. This material has air-like electrical characteristics (ε_r = 1.05 @ 2.5 GHz, 1.043 @ 5 GHz, 1.046 @ 10 GHz) and its purpose was to keep the antenna-body distance constant, as well as to minimize the body effect on the antenna characteristics. Since four positions were selected, both forward and reverse channels were measured, and each channel was swept 100 times, the number of channel frequency responses for the data analysis was 2400 for both antenna types. All antenna attachments were also photographed for further verifications of the measurement results.

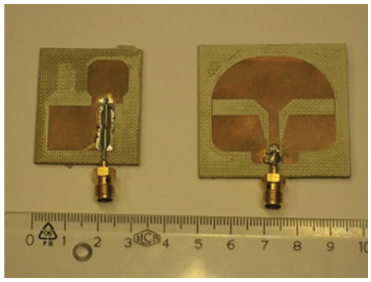

Figure 1. The dipole (left) and double loop (right) antennas.

Table 1. The test person parameters

	Test Person			
Parameter	**A**	**B**	**C**	**D**
Gender	Male	Male	Male	Female
Height [cm]	164	183	191	162
Mass [kg]	67	95	99	60
BMI	24.9	28.3	27.1	22.9

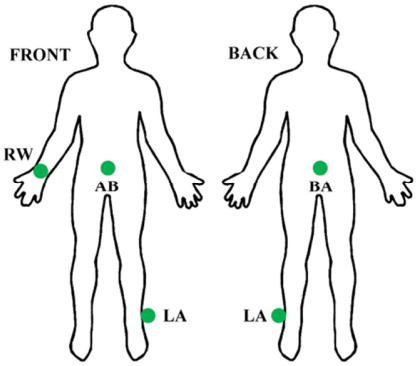

Figure 2. The selected antenna positions.

4. DATA POST-PROCESSING

The measured data describing the scattering parameters S_{21} of the radio links were post-processed with the MATLAB software. The frequency domain data was transformed into time domain CIRs by using the complex baseband inverse fast Fourier transform (IFFT) method [12], i.e., the IFFT algorithm was applied directly to the complex frequency domain data resulting complex CIRs to be used in the data analysis. No windowing functions were used. The achieved time resolution is the inverse of the measurement bandwidth 6 GHz: Δt = 0.167 ns.

5. RESULTS

5.1 First Arriving Paths

From the retrieved CIRs, the path losses of the first arriving signals were found out for each link. Based on the arrival time of the first arriving path, the corresponding distance was solved assuming that the signal is travelling at the speed of the light in the air, c. An interesting aspect must be considered when using this method for the distance extraction. Namely, when the VNA is calibrated, the zero time delay plane is transferred to the open ends of the measurement cables. When the antennas are attached to the cables, the signal has to travel in the antenna structure before entering into the air. This causes delay due to the antennas' physical dimensions. Secondly, the propagation speed in the antenna structure is [13]

$$v = \frac{c}{\sqrt{\varepsilon_r}}, \tag{2}$$

where ε_r is the relative permittivity of the substrate of the antennas, i.e., lower than the velocity of light. These two factors present both at the transmit and the receive antennas, have the effect that the distances appear to be longer than in reality. The distance errors must be compensated, since it may have significant

influence on the results in short radio links, as is the case with on-body communications. The error correction for the antennas used in this work is explained in detail in [5], where the mean errors were found to be 90 mm and 109 mm for the dipole and double loop antenna pairs, respectively.

In [5], path loss models using the same antennas as used here were solved according to the equation:

$$PL(d) = PL(d_0) + 10n\log_{10}\left(\frac{d}{d_0}\right) + S \ \ [\mathrm{dB}], \qquad (3)$$

where PL is the path loss in dB at a distance of d, $PL(d_0)$ is the path loss at the reference distance d_0, n is the path loss exponent and S is a random scattering term with a standard deviation of σ. The values of n = 3.3 and 2.7, $PL(d_0)$ = 31.6 dB and 39.8 dB whereas σ = 12.8 dB and 13.8 dB were found out for the dipole and double loop antennas, respectively. For d_0, a value of 50 mm was used. After solving the link distances from the CIRs in this paper, the path losses predicted by (3) were calculated.

Fig. 3 shows the results for the dipole antenna for different persons by applying the ideas of quantile-quantile (QQ) plots [14]. The graphs in Fig. 3 are not true QQ plots, since they do not base on distributions as the classical QQ plots. However, these QQ-like plots provide a convenient and illustrative tool to examine how the measured data follows the mathematical model. In the horizontal axis, the path loss values are calculated using (3) whereas the vertical axis shows the measured values. The blue line describes the case, if the measured values were exactly the same as predicted by (3) assuming S = 0. The dotted black lines denote the limits for σ. The red circles show the measured path losses for the six links, where each point contains the average value of the forward and reverse links under consideration. If the measured value is between the standard deviation lines, it follows the model in (3). If the point is above the blue line, the model underestimates the path loss and vice versa. Between the male test persons A, B and C, the model works best for the person B, since four measurements follow the model, whereas for A and C cases three points lie between the standard deviation lines. For the female person D, four dots reach the model. For all persons, two results that are beyond the model have a larger path loss than predicted. The points present the links AB-BA and RW-BA. In the measurements in [5], the position BA was not present. Thus the link types of the outliers in Fig. 3 were missing explaining the deviation from (3). For persons B and C, the model overestimates the path loss for four links, for person D underestimates for four links and for person A three links are underestimated. Visually observed, the model follows best the dots of the person D.

Fig. 4 shows the QQ-like plots for the double loop antenna. For the persons B, C and D, five links follow the model, for the person A only two. The model seems to operate better with the double loop antenna case. The differences between the persons originate from many reasons. The link types are very heterogeneous having different propagation mechanisms as creeping waves, diffraction and waves travelling in air. The body shapes vary between the sizes and the gender of the persons. Finally, it is very difficult to place the persons in exactly similar body postures, causing large differences in shadowing, especially for the links with an antenna on the wrist and ankle.

The bar diagrams in Fig. 5 describe the measured path losses and the corresponding link distances for the dipole antennas. The link

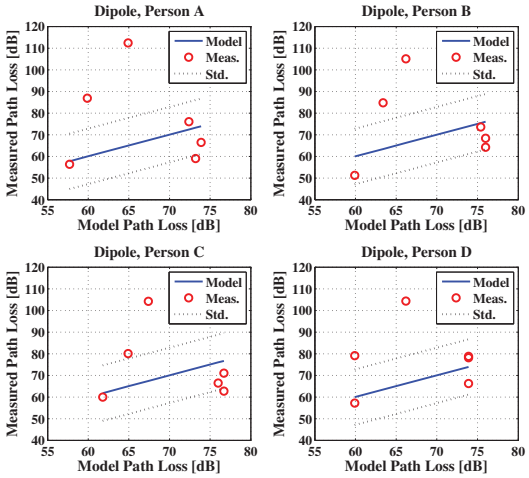

Figure 3. QQ-like plots for the dipole antenna.

acronyms between the subplots refer both to the path losses in the upper plot and the distances below.The link distances increase as the body size of the test person is increased. The path losses do not show a common trend. For example, for the AB-BA, RW-LA and LA-BA links the loss decreases as the body size is increased for the persons A, B and C. With the LA-BA-link, the opposite is true. Similar types of observations are reported in [15]. The comparison between genders, i.e., persons A and D, shows higher loss for the female in the links LA-BA and AB-LA explained by the differences of the body shapes and compositions of the genders as the signal is travelling along the body surface. For the link AB-RW on the other hand, the loss is approximately the same since the signal travels mainly in the air experiencing similar propagation conditions for both genders.

Fig. 6 shows the corresponding results for the double loop. They in general follow the same patterns as with Fig. 5. For AB-LA and LA-BA, the loss increases as the body size is increased for the males, for the RW-LA it is decreased. The AB-RW shows no noticeable difference between the body sizes or genders. The path loss differences between the test persons are typically roughly within 10 dB and at the maximum within 20 dB.

Fig. 7 shows the results when the distance dependency of the path losses is removed by solving the value of n in (3) by inserting the measured values of d and $PL(d)$, the model values of d_0 and $PL(d_0)$ from [5], and assuming S = 0. Also the modelled path loss exponent from [5] is shown for both antennas. It can be noted by comparisons of Figs. 5, 6 and 7 that if the persons are listed in an ascending order of measured values of n and the measured absolute path losses, the order is for most of the links the same. This means, that the variance in the results between the persons originates mostly from the differences in the body shapes, compositions and body postures. The links AB-BA and RW-BA show high exponent values, due to the creeping wave propagation around the body curvature and strong shadowing, respectively. Table 2 shows the average values for the path loss exponents for both antennas. The average exponent is noted to decrease as the body size is increased between the persons A, B and C. The male-female comparison, A vs. D, shows that no difference exists in n between the genders with similar body sizes. However, as noted above, differences in separate links do exist.

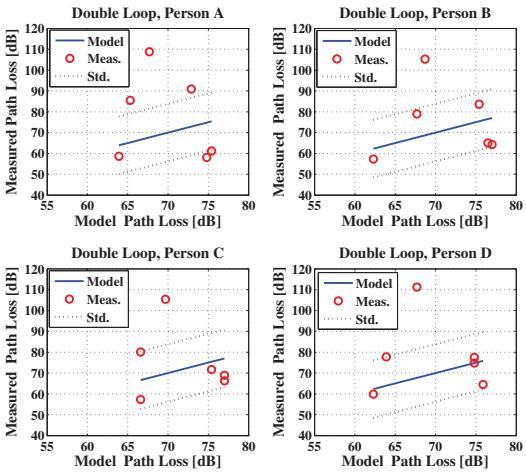

Figure 4. QQ-like plots for the double loop antenna.

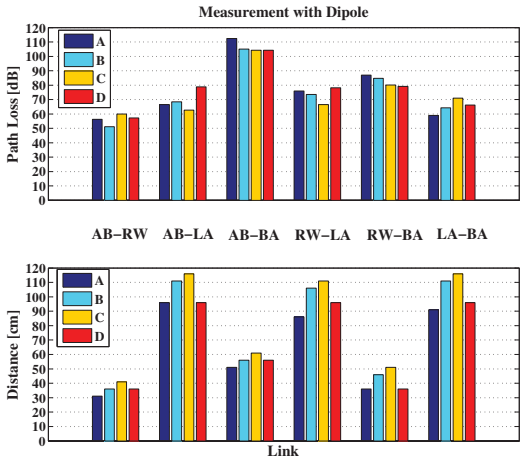

Figure 5. Path losses and link distances for the dipole.

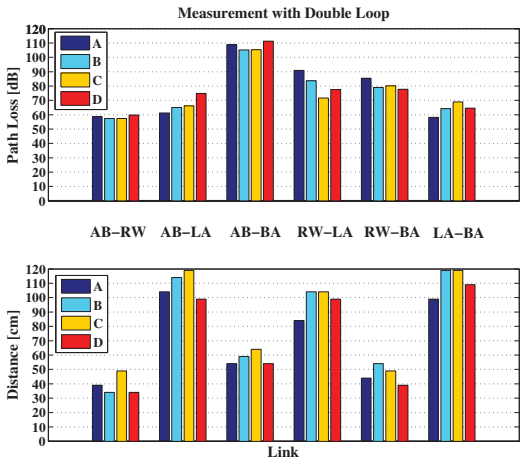

Figure 6. Path losses and link distances for the double loop.

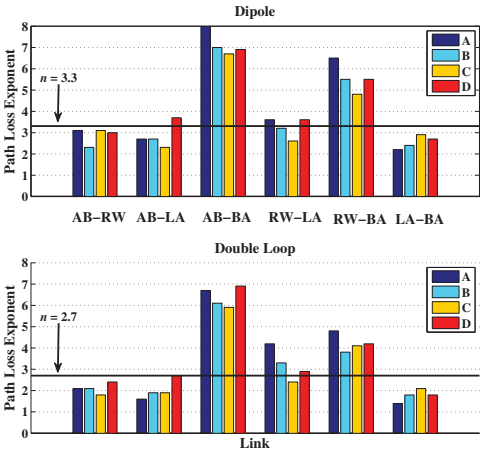

Figure 7. Path loss exponents of the links.

Table 2. Average path loss exponents (*n*)

	Test Person			
	A	**B**	**C**	**D**
Dipole	4.3	3.9	3.7	4.2
Double Loop	3.5	3.2	3.0	3.5

5.2 Excess Delays

The Federal Communications Commission (FCC) has set an upper limit of −41.3 dBm/MHz for the power spectral density between the frequency band of 3.1-10.6 GHz for indoor communications [16]. In the IEEE standard [4], a single UWB channel is defined to have a bandwidth of 499.2 MHz. Therefore the maximum transmit power within a single channel is limited to −14.3 dBm. The same standard sets the receiver sensitivity demand to be −76… −91 dBm depending on the selected data rate for an on-off keyed UWB system. The values assume a 10 dB noise figure and 5 dB implementation loss. Should the noise figures and implementation losses be smaller than these, an additional 5 dB margin is applied in the excess delay analysis. As a result, the threshold for the maximum allowable path loss is set to −82 dB, as was done in [7]. The excess delays of the measured channels are solved from the average CIRs. Fig. 8 shows the number of taps in the CIRs describing the excess delay for each antenna, link and person. It is noted that also here a large variation exists depending on the link and person under consideration. In the link AB-BA, the number of CIR taps is zero describing the case when no signal was detected above the threshold level of −82 dB. The same applies to the RW-LA link for the persons A and D with the dipole, to the RW-BA link for the person A with both antennas and for the person B with the dipole. Especially the AB-BA channel seems to be useless for a communication unless, e.g., relaying technique is applied. Very bad links have longer excess delays with larger males than small. In the gender comparison, A vs. D, longer excess delays are noted for the female in seven cases, in three cases the male's CIRs have more taps. In the cases of RW-BA (dipole) and RW-LA (dipole and loop) the link is operable with the female, but not with the male. The results depend heavily on the body postures, as noted with the first path analysis. The mean values of CIR tap numbers calculated from

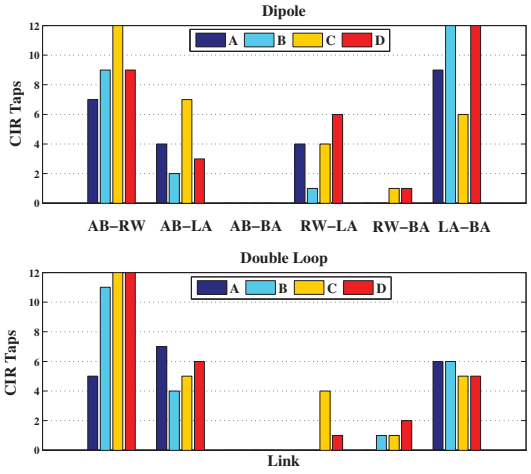

Figure 8. Number of taps in the CIRs.

Fig. 8 are 3.5, 3.8, 4.8 and 4.8 for the persons A, B, C and D, respectively. Thus a comparison between the males results longer excess delays as the person size increases. On the other hand, the female has similar result with the largest male. Comparison between the antennas gives mean CIR tap values 5.2 and 4.2 for the dipole and double loop. On the average, the dipole results longer CIR above the detection threshold.

5.3 Channel Correlations

Cross-correlations (CC) between the channel pairs were calculated by using the equation [17]

$$r_{h_i h_j}(l) = \sum_{n=-\infty}^{\infty} h_i(n) h_j(n-l)\,, \qquad (4)$$

where l = 0, ±1, ±2,… and h_i and h_j are the CIRs of the two channels. The CIRs were aligned in time so that the first arriving path is the first sample in each CIR. The CIRs were cut to the length of 50 samples. The energy of the CIRs was normalized to unity, thus giving the maximum value of one for a CC. From the resulting cross-correlation function, the maximum value was selected to represent the correlation. The CCs were solved for all link pair combinations, 15 altogether, that are listed in Table 3. From the practical perspective, the pairs 1, 2 and 6 may be the most interesting, since quite often it is assumed that AB would be the central node through which all other nodes communicate. For a larger view, all CCs were found out.

Fig. 9 presents the CCs for all link pairs, persons and both antennas. A rough division into two categories is noted: in general, the link pairs 2, 6, 10, 11 and 12 show a lower correlation level, under 0.7, than the rest of the cases. However, all these cases contain the link AB-BA, which was noted to be unsuitable for use in Fig. 8 due to too high path loss. Therefore, although low correlation values would be beneficial, e.g., at applying ideas of the spatial diversity, in this case the link pairs with low CC values are in practice unusable.

Table 4 shows the result when the differences of the CCs are calculated between different pairs of persons based on Fig. 9. For instance, the case A vs. B is obtained by subtracting the CCs of

Table 3. Link pairs for the correlation calculation

No.	Link Pairs	No.	Link Pairs	No.	Link Pairs
1	AB-RW/AB-LA	6	AB-LA/AB-BA	11	AB-BA/RW-BA
2	AB-RW/AB-BA	7	AB-LA/RW-LA	12	AB-BA/LA-BA
3	AB-RW/RW-LA	8	AB-LA/RW-BA	13	RW-LA/RW-BA
4	AB-RW/RW-BA	9	AB-LA/LA-BA	14	RW-LA/LA-BA
5	AB-RW/LA-BA	10	AB-BA/RW-LA	15	RW-BA/LA-BA

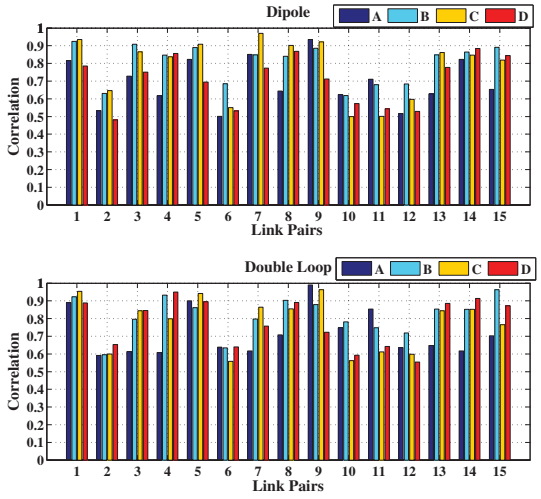

Figure 9. Correlations between the links.

Table 4. Sign distribution of the correlation differences

		Compared Persons			
		A vs. B	B vs. C	A vs. C	A vs. D
Dipole	Positive	11	7	12	8
	Negative	4	8	3	7
Double Loop	Positive	11	6	10	9
	Negative	4	9	5	6
Both	Positive	22	13	22	17
	Negative	8	17	8	13

the person A from the CCs of the person B for each link pair. Then the numbers of positive and negative values are summed up. For A vs. B it is noted that the values are mostly positive. Thus, the larger test person has higher CC values than the smaller one. This is verified by the case A vs. C. The case B vs. C shows much more evenly distributed signs especially for the dipole antenna, since the relative body size difference between B and C is much smaller than with A vs. B. The gender comparison A vs. D results a similar kind of observation: the test persons have similar body sizes thus giving evenly distributed signs, especially for the dipole. The gender seems not to have a clear effect on the CCs.

6. CONCLUSIONS AND FUTURE WORK

The effect of the human body size and gender on the UWB on-body WBAN radio channels was examined. The work is based on

static frequency domain measurements at 2-8 GHz frequency range in an anechoic chamber using three male test persons and one female. The measurements were repeated by using two antenna types: dipole and double loop. The data was post-processed to obtain the time-domain CIRs for the analysis.

Firstly, the first arriving paths of the CIRs were investigated. A previously developed path loss model and the measured values were compared. It was noted that for the female, the results obeyed the model best. No clear difference between the males was noted. The double loop results followed the path loss model better than the dipole case. The comparison of the measured absolute path losses showed large variations between the links and persons. In some cases the increasing body size caused an increase in the path loss, in some cases the opposite. This is explained by the heterogeneity of the links, having different signal propagation mechanisms and also differences in body postures during the measurements. When the distance dependency in the path losses was removed, it was noted that the variance of the results between the persons originated mostly from the differences between the body shapes, postures and compositions: The differences in the link distances between the persons with different body sizes did not have as large effect. Examination of the path loss exponents showed a decrease as the body size was increased. No difference existed between the genders with the same body sizes.

Secondly, the excess delays of the CIRs were solved out. It was noted, that the link between the abdomen and back is unusable for communication unless, e.g., relaying techniques is used. The largest observed value of the excess delay was 12 taps. The mean value of the taps was noted to increase as the body size increases among the males. The result of the female had similar value as the largest male. Comparison between the antennas showed longer excess delay for the dipole antenna.

Thirdly, the cross-correlations between the CIRs were solved by forming 15 combinations of link pairs. On the average the correlation values increased with the larger body size. No difference was noted between the genders of the same size.

The results varied heavily between the channels since the link types and the propagation mechanisms are different. Also the limb positions and the body shapes have a strong effect on the observations. As a further work, more measurements are needed with a larger number of test persons and measurement points to average out the effect of variations in the channel conditions.

7. ACKNOWLEDGMENTS

The work was partly funded by the Finnish Funding Agency for Technology and Innovation (Tekes) by the project Wireless Body Area Network for Health and Medical Care (WiBAN-HAM).

8. REFERENCES

[1] United Nations, Department of Economic and Social Affairs, (May 2014), [Online]. Available: http://www.un.org/en/development/desa/population/publications/pdf/ageing/2012PopAgeingandDev_WallChart.pdf.

[2] Hämäläinen, M., and Kohno, R. 2007. Prospects for wireless technology in remote care processes. In *Proceedings of the 2nd International Symposium on Medical Information and Communication Technology* (Oulu, Finland, December 11-13, 2007). ISMICT 2007. 1-4.

[3] Hall, P. S., and Hao, Y. 2012. *Antennas and Propagation for Body-Centric Wireless Communications, 2nd ed*. Artech House, Norwood, MA, USA.

[4] IEEE standard for local and metropolitan area networks, IEEE 802.15.6-2012 – Part 15.6: Wireless Body Area Networks. 2012.

[5] Kumpuniemi, T., Tuovinen, T., Hämäläinen, M., Yekeh Yazdandoost, K., Vuohtoniemi, R., and Iinatti, J. 2013. Measurement-based on-body path loss modelling for UWB WBAN communications. In *Proceedings of the 7th International Symposium on Medical Information and Communication Technology* (Tokyo, Japan, March 6-8, 2013). ISMICT 2013. IEEE, 233-237. DOI= http://dx.doi.org/10.1109/ISMICT.2013.6521735.

[6] Kumpuniemi, T., Hämäläinen, M, Tuovinen, T., Yekeh Yazdandoost, K., and Iinatti, J. 2013. Generic small scale channel model for on-body UWB WBAN communications. In *Proceedings of The Second Ultra Wideband for Body Area Networking Workshop. Co-located with the 8th International Conference. on Body Area Networks* (Boston, USA, September 30-October 2, 2013). UWBAN-2013, BodyNets-2013. ICST 570-574. DOI= http://dx.doi.org/10.4108/icst.bodynets.2013.253673.

[7] Kumpuniemi, T., Hämäläinen, M., Tuovinen, T., Yekeh Yazdandoost, K., and Iinatti, J. 2014. Radio channel modelling for pseudo-dynamic WBAN on-body UWB links. In *Proceedings of the 8th International Symposium on Medical Information and Communication Technology* (Florence, Italy, April 2-4, 2014). ISMICT 2014. IEEE. DOI= http://dx.doi.org/10.1109/ISMICT.2014.6825227.

[8] Tuovinen,T., Kumpuniemi, T., Yekeh Yazdandoost, K., Hämäläinen, M., and Iinatti, J. 2013. Effect of the antenna-human body distance on the antenna matching in UWB WBAN applications. In *Proceedings of the 7th International Symposium on Medical Information and Communication Technology* (Tokyo, Japan, March 6-8, 2013). ISMICT 2013. IEEE 193-197. DOI= http://dx.doi.org/10.1109/ISMICT.2013.6521727.

[9] Tuovinen, T., Kumpuniemi, T., Hämäläinen, M., Yekeh Yazdandoost, K., and Iinatti, J. 2013. Effect of the antenna-body distance on the on-ext and on-on channel link path gain in UWB WBAN applications. In *Proceedings of the 35th Annual International Conference of the IEEE Engineering in Medicine and Biology Society* (Osaka, Japan, July 3-7, 2013). EMBC 2013. IEEE 1242-1245. DOI= http://dx.doi.org/10.1109/EMBC.2013.6609732.

[10] World Health Organization (WHO). Global Database on Body Mass Index, (May 2014), [Online]. Available: http://apps.who.int/bmi/index.jsp?introPage=intro_3.html.

[11] Rohacell. (June 2014), [Online]. Available: http://www.rohacell.com/product/rohacell/en/products-services/rohacell-hf/pages/default.aspx.

[12] Denis, B., and Keignart, J. K. 2003. Post-processing framework for enhanced UWB channel modeling from band-limited measurements. In *Proceedings of the 2003 IEEE Conference on Ultra Wideband Systems and Technologies* (Reston, USA, November 16-19, 2003). UWBST 2003. IEEE 260-264. DOI= http://dx.doi.org/10.1109/UWBST.2003.1267844.

[13] Pozar, D. M. 2005. *Microwave Engineering, Third Edition*. John Wiley & Sons Inc, Danvers, MA, USA.

[14] Thode, H. C. 2002. *Testing for Normality*. Marcel Dekker, New York, NY, USA.

[15] Khan, M. M., Rahman, Md. A., Alomainy, A., and Parini, P. 2013. Ultra wideband on-body radio radio propagation channels study for different real human test subjects with various sizes and shapes. In *Proceedings of the 2013 International Conference on Advances in Electrical Engineering* (Dhaka, Bangladesh, December 19-21, 2013). ICAEE 2013. IEEE 323-328. DOI= http://dx.doi.org/10.1109/ICAEE.2013.6750357.

[16] Allen, B., Dohler, M., Okon, E. E., Malik, W. Q., Brown, A. K., and Edwards D.J. (editors). 2007. *Ultra-wideband Antennas and Propagation for Communications, Radar and Imaging*. John Wiley & Sons, Chichester, West Sussex, England.

[17] Proakis, J. G., and Manolakis, D. G. 1996. Digital Signal Processing, Principles, Algorithms and Applications, Third Edition. Prentice-Hall, Upper Saddle River, NJ, USA.